Q-ball scattering on barriers and holes in one and two spatial dimensions

2009 J. Phys. A: Math. Theor. 42 245201

(http://iopscience.iop.org/1751-8121/42/24/245201)

IOP PUBLISHING JOURNAL OF PHYSICS A: MATHEMATICAL AND THEORETICAL

J. Phys. A: Math. Theor. **42** (2009) 245201 (22pp) doi:10.1088/1751-8113/42/24/245201

Q-ball scattering on barriers and holes in one and two spatial dimensions

Jassem H Al-Alawi and Wojtek J Zakrzewski

Department of Mathematical Sciences,University of Durham, Durham DH1 3LE, UK

E-mail: J.H.Al-Alawi@durham.ac.uk and W.J.Zakrzewski@durham.ac.uk

Received 25 February 2009, in final form 24 April 2009
Published 26 May 2009
Online at stacks.iop.org/JPhysA/42/245201

Abstract

We discuss various scattering properties of non-topological solitons, *Q*-balls, on potential obstructions in $(1+1)$ and $(2+1)$ dimensions. These obstructions, barriers and holes, are inserted into the potential of the theory via the coupling parameter, i.e. $\tilde{\lambda}$, that is effective only in a certain region of space. When $\tilde{\lambda} > 1$ the obstruction is a barrier and when $0 < \tilde{\lambda} < 1$ the obstruction is a hole. The dynamics of *Q*-balls on such obstructions in $(1+1)$ dimensions is shown to be very similar to that of topological solitons provided that the *Q*-balls are stable. In $(2+1)$ dimensions, numerical simulations have shown some differences from the dynamics of topological solitons. We discuss these differences in some detail.

PACS numbers: 03.75.LM, 05.45.Yv

1. Introduction

Motivated by our earlier work on the scattering of topological solitons on potential obstructions in a class of models [1, 2] we have decided to look at the generality of these results. To do this we have decided to investigate the scattering properties of non-topological solitons so in this paper we look at the scattering of *Q*-balls on various potential obstructions. In fact other studies of the effects due to inhomogeneities, within the framework of perturbation theory of solitons, have also been carried out (see e.g. [3–5]).

First we recall that *Q*-balls are non-topological soliton fields, first introduced by Coleman in [6]. They arise in some classes of self-interacting complex scalar fields. Unlike topological solitons, whose stability is ensured by the presence of a conserved topological charge, *Q*-balls carry a conserved Noether charge associated with the global $U(1)$ symmetry. This conserved but non-topological charge stabilizes the *Q*-balls. Also, *Q*-balls have a time-dependent rotating phase and the conserved Noether charge is related to the velocity of the change of this phase. These features result in a much more complicated scattering properties of these solitons, leading to such phenomena as, for example, the charge fission during the scattering process.

In this paper we investigate the Q-ball dynamics in $(1+1)$ and $(2+1)$ dimensions, mainly when the Q-balls are scattered on various obstructions in the form of potential barriers or holes. First we discuss the conditions of the stability of the Q-balls. Then we report the results of our numerical simulations which have revealed that Q-balls behave like topological solitons only for the values of the parameters of the theory that guarantee this stability throughout the scattering. When this condition is satisfied the dynamics of the scattering on barriers and holes in $(1+1)$ dimensions is similar to what was seen for topological solitons [1, 2], i.e. very little radiation is given off during the scattering. The scattering on barriers results in transmission or reflection, i.e. very much like that of a small particles. In the scattering on holes, like for topological solitons, we can have transmissions, trappings and reflections. As discussed before [1, 2, 7, 8] the trappings correspond to the case of solitons which, while in the hole, lose energy through radiation and the reflections correspond to the very coherent interaction of solitons with this radiation. We find similar properties of the scattering of Q-balls except that this time they also generate further small Q-balls. This scattering is discussed in detail in sections 3 and 4.

In section 5, we discuss the scattering of solitons in $(2+1)$ dimensions. We find that, again, the scattering often resembles the scattering of small particles but the properties of this scattering depend crucially on the parameters of the theory. However, there are also small differences which we discuss in detail. The paper ends with a short section presenting our conclusions.

2. Q-balls in D spatial dimensions

We consider a complex scalar field Φ in D spatial dimensions [9] whose Lagrangian density is given by

$$\mathcal{L} = \tfrac{1}{2}\partial_\mu \Phi \partial^\mu \Phi^* - U(|\Phi|), \tag{1}$$

where the indices μ and ν run from 0 to D. The energy–momentum tensor takes the form:

$$T_{\mu\nu} = \partial_\mu \Phi \partial_\nu \Phi^* - g_{\mu\nu}\mathcal{L}, \tag{2}$$

where $g_{\mu\nu}$ is the spacetime metric with signature $(+,-,-\ldots)$. This Lagrangian has been so chosen that it is invariant under the global $U(1)$ transformation and the conserved Noether current, j^μ, associated with this symmetry, is given by

$$j^\mu = \frac{1}{2\mathrm{i}}(\Phi^* \partial^\mu \Phi - \Phi \partial^\mu \Phi^*), \tag{3}$$

The corresponding conserved Noether charge, Q, is then

$$Q = \int j^0 \, \mathrm{d}^D x. \tag{4}$$

The total energy and momentum are given, respectively, by

$$E = \int T_{00} \, \mathrm{d}^D x, \tag{5}$$

$$P_i = \int T_{0i} \, \mathrm{d}^D x, \tag{6}$$

where i is the spatial index which runs from 1 to D.

The stationary Q-ball located at the origin is described by

$$\Phi = \mathrm{e}^{\mathrm{i}\omega t} f(r), \tag{7}$$

where ω is the internal rotation frequency and $f(r)$ is the real radial profile function which satisfies the equation of motion which follows from (1), namely:

$$\frac{\mathrm{d}^2 f}{\mathrm{d}r^2} = \frac{(1-D)}{r}\frac{\mathrm{d}f}{\mathrm{d}r} - \omega^2 f + U'(f), \tag{8}$$

where D is the number of spatial dimensions.

For the consistency of the equations and in order that the Q-ball has a finite energy, the profile function f, has to satisfy the following boundary conditions:

$$\frac{\mathrm{d}f(0)}{\mathrm{d}r} = 0 \tag{9}$$

and

$$f \to 0 \qquad \text{as} \quad |r| \to \infty. \tag{10}$$

The corresponding field (7) is then called the stationary Q-ball.

As the Lagrangian (1) is Lorentz invariant the field (7) can be boosted with any velocity up to the speed of light.

Note that the equation for f, (8), can be treated as a mechanical analogue describing a point particle moving in an effective potential with friction if f is interpreted as the position of the particle and r as the time coordinate [9]. The effective potential in which this particle moves is then

$$U_{\text{eff}}(f) = \tfrac{1}{2}\omega^2 f^2 - U(f). \tag{11}$$

The 'friction' term $\frac{1-D}{r}$ becomes important for high D or small r.

2.1. Q-balls in (1 + 1) *dimensions*

First let us choose our potential $U(f)$. We want it to be such that it gives rise to an exact Q-ball solution in (1 + 1) dimensions. This potential should have an absolute minimum when $U(0) = 0$. Then $\Phi = 0$ would be the ground state of the theory. Moreover, we require that the symmetry of the theory remains unbroken.

However, looking at (11) we note that there are further conditions on the parameters of the Q-ball (i.e. ω). To see this we observe that the Q-ball field exists provided that $f = 0$ corresponds to a local maximum of the effective potential i.e. $U''_{\text{eff}}(0) = [2U/f^2]_{f=0} < 0$. This leads to an upper bound on the frequency $\omega = \omega_+$. Also, the local minimum of $[2U(f)/f^2]$ must be attained at some positive value of $f = f_0$ and this requirement puts a lower bound on ω i.e. $\omega = \omega_-$,

$$\left[2U(f_0)\big/ f_0^2\right] < \omega < U''(0). \tag{12}$$

Thus the Q-ball field exists for ω in this range, i.e. $\omega_- < \omega < \omega_+$. Of course, as (11) is quadratic in ω, we can also take negative values of ω—the corresponding fields are called anti-Q-balls. However, the existence of a Q-ball does not guarantee its stability. For a Q-ball field configuration to be stable we have to require that $E(Q) < mQ$, where m is the mass of the scalar field.

The potential we have chosen to use has the form [10]:

$$U(|\Phi|) = 2|\Phi|^2 - 2|\Phi|^4 + |\Phi|^6. \tag{13}$$

With this potential Q-ball solutions exist for $\sqrt{2} < \omega < 2$. Moreover, these Q-balls are stable as $m = 2$.

Next we insert our obstructions. Following our earlier work [1, 2] on the soliton scattering on obstructions we introduce a potential parameter that perturbs the Q-ball only

in a certain region of space. The Q-ball, as it moves towards this region, will only experience this perturbation when its profile function f is non-zero in this region. We introduce the perturbation in the form of potential barriers and holes, and hence we modify the potential $U(\Phi)$ to become

$$\tilde{U}(|\Phi|) = \tilde{\lambda} U(|\Phi|), \tag{14}$$

in which $\tilde{\lambda} = 1 + \lambda(x)$.

Thus $\lambda(x)$ is the extra potential parameter which has been inserted into the potential $\tilde{U}(|\Phi|)$ to take into account the effects of obstructions, holes and barriers, and so is non-zero only in a certain region of space.

In our case, we have put the obstruction around the origin (i.e. $x = 0$) and so we have taken

$$\lambda(x) = \begin{cases} 0 & |x| > 10 \\ \lambda_0 = \text{constant} & |x| \leqslant 10. \end{cases}$$

The Q-ball in our model is really quite sizeable (i.e. the solution to (8) for the potential (13) is nonzero for a sizeable region of x) so the obstruction has been made quite large to make sure that the Q-ball size fits into it quite easily; i.e. is significantly larger than the size of the Q-ball.

The equation of motion, in the presence of the obstruction, now takes the form

$$\ddot{\Phi} - \Phi'' + 2\Phi\tilde{\lambda}(2 - 4|\Phi|^2 + 3|\Phi|^4) = 0. \tag{15}$$

Using the Q-ball ansatz, the field equation for the profile function, $f(x)$ now takes the form:

$$f'' + (\omega^2 - 4\tilde{\lambda}) + 8\tilde{\lambda} f^3 - 6\tilde{\lambda} f^5 = 0. \tag{16}$$

This profile equation (16) can only be solved exactly when $\lambda(x) = \lambda_0 = \text{constant}$. Then with the help of [11] we note that f is given by

$$f(x) = \left(\frac{1}{\tilde{\lambda}}\right)^{\frac{1}{4}} \left[\frac{4\tilde{\lambda} - \omega^2}{2\sqrt{\tilde{\lambda}} + \sqrt{2\omega^2 - 4\tilde{\lambda}}\cosh\left(2x\sqrt{4\tilde{\lambda} - \omega^2}\right)}\right]^{\frac{1}{2}}. \tag{17}$$

As the theory is Lorentz invariant this solution can be boosted or shifted by a spatial translation. Then, the Q-ball solution becomes

$$f(x) = \left(\frac{1}{\tilde{\lambda}}\right)^{\frac{1}{4}} \left[\frac{4\tilde{\lambda} - \omega^2}{2\sqrt{\tilde{\lambda}} + \sqrt{2\omega^2 - 4\tilde{\lambda}}\cosh\left(2\gamma\sqrt{4\tilde{\lambda} - \omega^2}(x - x_0 - ut)\right)}\right]^{\frac{1}{2}} \tag{18}$$

where x_0 is the position of the Q-ball, u its velocity and γ is the usual relativistic factor.

However, $\tilde{\lambda} \neq$ constant and so this expression does not solve (16) for all values of the parameters. On the other hand our $f(x)$, (18), is strongly localized and so if the Q-ball is far away from the obstruction the solution to (16) is approximately given by (18) and so (18) can be used for the initial condition of our numerical simulation of (15).

Note that when the Q-ball is far enough from the obstruction $\tilde{\lambda} = 1.0$ and (18) becomes

$$f(x) = \left[\frac{4 - \omega^2}{2 + \sqrt{2\omega^2 - 4}\cosh\left(2\gamma\sqrt{4 - \omega^2}(x - x_0 - ut)\right)}\right]^{\frac{1}{2}} \tag{19}$$

The associated Q-ball Noether charge and the energy become

$$Q = \omega\gamma I_2 \tag{20}$$

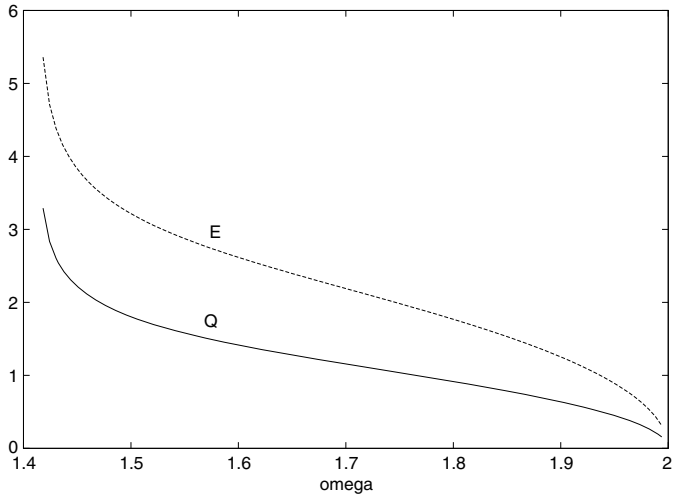

Figure 1. The energy E_ω and the charge Q_ω as a function of ω.

$$E = \tfrac{1}{2}\gamma^2(u^2+1)I_x + \tfrac{1}{2}\omega^2\gamma^2(u^2+1)I_2 + 2I_2 - 2I_4 + I_6, \tag{21}$$

where

$$I_2 = \int_{-\infty}^{\infty} f^2\,\mathrm{d}x = \sqrt{2}\omega\tanh^{-1}\left[\frac{2-\omega'}{2+\omega'}\right]^{\frac{1}{2}} \qquad \text{and} \qquad \omega' = \sqrt{2\omega^2-4}.$$

Moreover,

$$I_4 = \int_{-\infty}^{\infty} f^4\,\mathrm{d}x = -\frac{4-\omega^2}{2} + I_2,$$
$$I_6 = \int_{-\infty}^{\infty} f^6\,\mathrm{d}x = \frac{-3\sqrt{4-\omega^2}}{4} + \frac{(\omega^2+2)}{4}I_2,$$
$$I_x = \int_{-\infty}^{\infty} f'^2\,\mathrm{d}x = \frac{4-\omega^2}{2} - \frac{\omega'^2}{4}I_2.$$

We see that both Q and E depend on ω and so, in follows, we call them Q_ω and E_ω.

Thus the Q-ball Noether charge is

$$Q_\omega = \sqrt{2}\omega\gamma\tanh^{-1}\left[\frac{2-\omega'}{2+\omega'}\right]^{\frac{1}{2}} \tag{22}$$

and the energy becomes

$$E_\omega = \frac{1}{4}\left(\gamma^2(u^2+1)+1\right)\left[\sqrt{4-\omega^2} + (\omega^2+2)\frac{Q_\omega}{\omega}\right]. \tag{23}$$

When $u = 0$ (i.e. the Q-ball is at rest) the energy becomes its mass and is given by

$$M_\omega = \frac{\sqrt{4-\omega^2}}{2} + \frac{(\omega^2+2)}{2}\frac{Q_\omega}{\omega}. \tag{24}$$

Looking at these formulae we observe that as $\omega \approx \omega_+$, Q_ω and $E_\omega \to 0$ and when $\omega \approx \omega_-$ then Q_ω and $E_\omega \to \infty$. Figure 1 shows that E_ω and Q_ω are monotonically decreasing functions of ω. Furthermore, as ω increases the charge decreases and in the limit

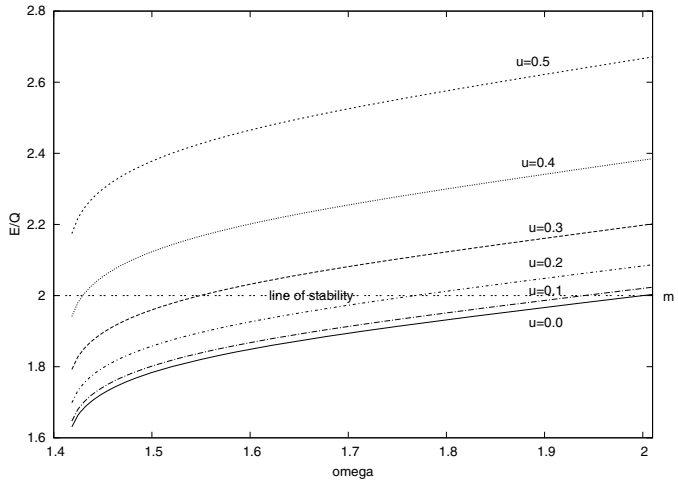

Figure 2. The energy–charge ratio E/Q as a function of ω for various velocities.

as $\omega \approx \omega_+$ the charge, $Q_\omega \to 0$. In this upper bound limit the energy–charge ratio approaches the mass of the scalar field, i.e. $m = 2$. In the lower bound limit, i.e. when $\omega \approx \omega_-$, the ratio $\frac{E_\omega}{Q_\omega} \to \omega_-$. Figure 2 shows clearly that the energy–charge ratio is below the mass term of the scalar field when the velocity of the Q-ball is small [12]. When $u = 0.0$ the energy–charge ratio is always below the stability line and only intersects this line when $\omega \sim \omega_+$. Thus, the Q-balls are stable for small velocities and so are prevented from decaying into a number of smaller Q-balls. However, when the Q-ball acquires higher speeds the absolute stability condition can be violated; Q-balls can still be long-lived and will, eventually, decay into a number of smaller Q-balls [10]. Figure 2 shows that as ω increases and so E_ω and Q_ω decrease the stability condition becomes more violated for higher velocities.

When an obstruction is present in a certain region of space the mass term gets modified by the perturbation factor $\tilde{\lambda}$, i.e. $m = 2\sqrt{\tilde{\lambda}}$. Thus, the stability line shown in figure 2 gets shifted and the amount of the shift depends on the magnitude of the perturbation. In the case of a barrier the stability line gets shifted upwards and downwards in the case of a hole. Consequently, the Q-ball is less stable in the presence of holes. This is what we have observed in our simulations.

This scattering on holes is very delicate since if we want the Q-ball to be stable against fission, as the Q-ball reaches the hole, the hole must be relatively shallow.

So, when the potential is lowered by a positive factor (but less than one), i.e. $0 < \tilde{\lambda} < 1$, the tail of the Q-ball may develop some small Q-balls in the hole even when the Q-ball has a vanishing velocity. On the other hand, the Q-ball stability is not affected by the height of the barrier in cases when the velocity is small. In fact, within some limits, the higher the barrier the more stable is the Q-ball scattering as the stability line is shifted further upwards. However, we have to be careful; the Q-ball may also become unstable if the barrier is too high.

One can also study the stability of the Q-ball at the scattering region where the obstruction is present (see e.g. [13, 14]).

In next two sections we discuss the dynamics of Q-balls as they meet an obstruction located around $x = 0$. In order to understand it we had to perform some numerical simulations. These simulations were performed using the fourth-order Runge–Kutta method of simulating the time

evolution. We used 12 001 points with the lattice spacing of $dx = 0.01$. Hence, the lattice extended from -60 to 60 in the x-direction. The time step was chosen to be $dt = 0.0025$. In our work we used the absorbing boundary conditions.

3. Q-ball scattering on barriers

When a Q-ball, or a topological soliton, is far away from an obstruction, to a good approximation, it can be treated as a point particle following a well-defined trajectory. However, when they approach the barrier the differences in their behaviour begin to arise. These differences stem from the fact that the Q-charge of the Q-ball is not quantized and that not only Q-balls exist only in a certain range of frequencies but also there are some conditions on the Q-ball that have to be satisfied for it to be stable. The work on topological solitons [1, 2, 7, 8] has revealed that the speed and the magnitude of the barrier do not affect significantly the general dynamics of the solitons. Topological solitons suffer some distortions during their scattering process but they do recover their original shape after the scattering as the scattering is quite elastic. For the Q-balls, however, their dynamics on obstructions (barriers or holes) is connected to their stability. And this stability depends on the velocity, the height of the obstruction and the internal frequency of the Q-balls and thus on their charge.

One major difference between the Q-balls and topological solitons as they scatter on barriers is their behaviour close to their critical velocities. Critical velocities of the solitons are the lowest velocities above which they can overcome the barrier and get transmitted and below which they are reflected. All models involving topological solitons that we have studied have shown that the solitons can be treated as point particles and that such a discussion leads to very accurate estimates of their critical velocity. There are no restrictions on the speed of the solitons or the height of the barrier. In the case of the Q-balls the situation is different. First of all, the critical velocity cannot be determined without having to impose some restrictions on their speeds and the height of the barrier. This is due to the possibility of the Q-ball becoming unstable during its interaction with the barrier.

As we have seen from figure 2 the stability condition is satisfied only for low velocities. When a barrier is present, the stability line is raised and more Q-ball field configurations become stable. So to begin with we will consider the scattering on very small barriers.

Before we go on and discuss the scattering dynamics of the Q-ball on such barriers, we have to determine whether the force between the Q-ball and the barrier is repulsive or attractive. To check this we have placed a Q-ball at rest close to the barrier. Figure 3 presents a trajectory of a Q-ball with $\omega = 1.9$ initially placed at rest at $x = -15$, i.e. five units of distance from a barrier of height 0.01. The plot clearly demonstrates that the Q-ball is repelled by the barrier. This repulsion is due to the tail of the Q-ball which interacts with the barrier. The further away we place Q-ball the smaller the tail and hence the weaker the repulsion but the repulsion is always there. So to study the scattering on the barrier we need to give the Q-ball a boost.

We have performed several simulations by boosting the Q-balls with various small velocities. All these simulations have shown that, like for the topological solitons, the scattering is very elastic. There is very little radiation sent out and although the shape of the Q-ball changes as it climbs the barrier—afterwards it returns to its original shape. Looking at the dependence on the frequency (i.e. Q) of the Q-ball we have noticed that the Q-balls of higher value of Q get closer to the barrier. However, when we tried to determine the velocity at which they reach the top of the barrier (i.e. the critical velocity) this dependence on the frequency disappears. Thus for a barrier of height 0.01 the numerically found value of $u_{\rm cr}$ was $u_{\rm cr} \sim 0.1$.

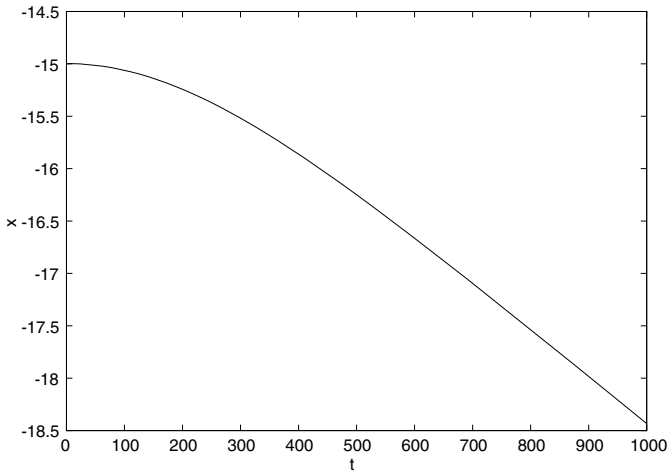

Figure 3. The trajectory of a Q-ball solution, $\omega = 1.9$, $u = 0$, placed at $x = -15$ from a barrier of 0.01 height.

As the scattering is very elastic we have tried to derive this value in the point particle approximation. In this case we look at the energy of the Q-ball at rest at the top of the barrier and compare it with the energy of a moving Q-ball away from the barrier. If the scattering is elastic the equality of these energies gives us a lower bound on the critical velocity.

Thus in our case

$$E_{\rm cr} \sim \frac{M_{\rm rest}}{\sqrt{1-u_{\rm cr}^2}}.$$

This energy should be very close to the rest mass energy of a Q-ball at the top of a barrier given by

$$E_{\rm cr} \sim M_B.$$

Thus the critical velocity is given by

$$u_{\rm cr} = \sqrt{1-\left(\frac{M_{\rm rest}}{E_{\rm cr}}\right)^2}. \tag{25}$$

So, let us use the above formula to estimate the critical velocity. The rest mass energy of the Q-ball with $\omega = 1.9$, far away from the potential barrier, is $M_{\rm rest} = 1.2528$ while its rest mass at the top of a barrier of height 0.01 is $E_{\rm cr} = 1.2591$. Thus,

$$u_{\rm cr} = \sqrt{1-\left(\frac{1.2528}{1.2591}\right)^2} = 0.0999,$$

which is in an excellent agreement with the numerical value mentioned before.

This was for the Q-ball of $\omega = 1.9$. What about other values? In table 1, we present the calculated critical velocities for several values of ω.

The agreement is clearly very good. This agreement shows that during the scattering very little radiation is sent out. Moreover, although the energies of the Q-balls depend on their frequency (i.e. on their charge Q) the value of the critical velocity is approximately independent of this frequency.

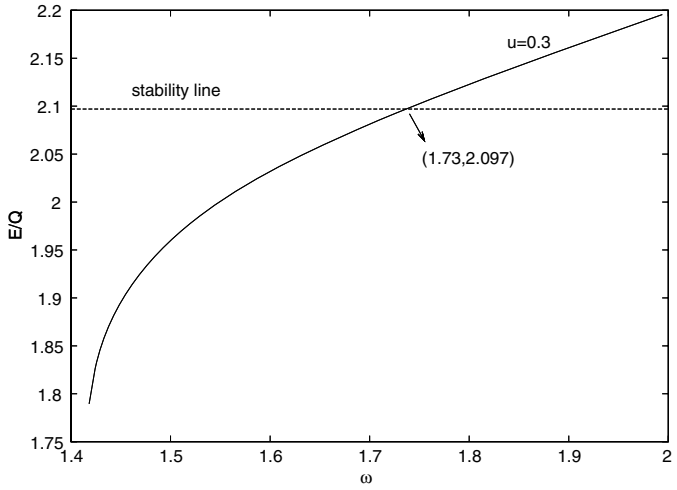

Figure 4. The stability line for a barrier of height = 0.1.

Table 1. Calculated dependence of M_{rest}, E_{cr} and u_{cr} on ω.

ω	M_{rest}	E_{cr}	u_{cr}
1.5	3.2159	3.231 99	0.099 38 $\sim$ 0.1
1.6	2.6167	2.629 85	0.0999 $\sim$ 0.1
1.7	2.1892	2.2002	0.0997 $\sim$ 0.1
1.8	1.7684	1.7772	0.0993 $\sim$ 0.1
1.9	1.2528	1.2591	0.0999 $\sim$ 0.1

We have also looked at barriers of different heights. In particular, when the height is 0.1 we have found that the critical velocity was around $\sim$0.3. Our estimates give us again the same value $\sim$0.3 but this time the stability line has increased to $m = 2.097$ (see figure 4) and so the Q-balls with frequency above $\omega = 1.73$ are unstable. Hence the barrier has divided the parameter space of Q-balls: only those with frequency below $\omega = 1.73$ are stable and for them the critical velocity is around $\sim$0.3.

What happens if we send a Q-ball which is unstable at the barrier?

We have performed such simulations and have found that such a Q-ball moves slower as it tries to climb the barrier and its tail gets distorted. When we repeated this experiment with higher barriers we have found that the Q-ball splits into two or more Q-balls. As the barrier is increased further the Q-ball splits into more Q-balls.

This fission starts at the edge of the barrier and the split off Q-balls are reflected while the parent Q-ball slowly climbs the barrier. At the time of splitting the Q-ball is quite distorted and this sets off the fission process. Note that this splitting depends on the frequency of the Q-ball as the Q-balls with low Q value are more likely to get deformed and so produce more fission during their scattering on the barrier.

Finally, let us examine the dependence of the repulsive force of the barrier on the frequency i.e. the charge of the Q-balls. To examine this we have placed two Q-balls (of frequencies $\omega = 1.5$ and $\omega = 1.9$), at rest, at $x = -15$ i.e. close to a barrier of height 0.9. In both cases, as expected, the Q-balls moved away from the barrier. However, the Q-ball with $\omega = 1.5$

has moved slower than the Q-ball with $\omega = 1.9$. Hence the forces acting on the Q-ball with $\omega = 1.5$ are weaker. This can be easily understood if we consider a Q-ball as a point particle and a barrier as a high wall. When two particles have the same momentum but one is more massive than the other one the momentum conservation implies that the massive one moves backwards slower than the less massive one. As the Q-ball with $\omega = 1.5$ is more massive than the one with $\omega = 1.9$ it moves away slower from the barrier.

If we decrease the height of the barrier, the Q-ball is repelled less. We have observed that the repulsive force between a Q-ball with $\omega = 1.9$ and a barrier of height 0.5 is less than the one with a height 0.9. So, the repulsive force decreases with the decrease of the height of the barrier.

It may appear somewhat surprising, at first sight, that the repulsive force between a barrier and a Q-ball depends on the charge while the critical velocity is independent of it. The Q-balls at the top of the barrier are modified by the scaling $\lambda \to \tilde{\lambda}$ and so we see that only the barrier height determines their critical velocity. We note that the mass of the Q-ball at the top of the barrier is scaled up so that $M_B = \sqrt{\tilde{\lambda}} M_{\rm rest}$. Hence, from (32), we see that the critical velocity is also a function only of the barrier height and is given by

$$u_{\rm cr} = \sqrt{\frac{\lambda_0}{1+\lambda_0}}. \tag{26}$$

Thus, when the height of the barrier is 0.01, the above expression gives for the critical velocity the value of 0.0995. Also, for a barrier of height 0.1 the above expression gives 0.3015. These results are in an excellent agreement with the values calculated and observed by us in our simulations.

4. Scattering of Q-balls on holes

The potential obstruction is a hole when $0 < \tilde{\lambda} < 1$. Then the potential is scaled down. While for the barriers the stability line (see figure 2) was shifted up—for holes it is shifted down and so the stability becomes more delicate. Interestingly, when the stability conditions of the Q-balls are satisfied, their scattering on the holes resembles the dynamics of topological solitons. Then a Q-ball far away from obstruction moves in a well-defined trajectory and as it encounters the hole it speeds up. If the Q-ball has enough energy it is transmitted giving off a small amount of radiation; otherwise it gets trapped in the hole.

As for holes the potential is scaled down, the corresponding stability line, i.e. the value of the mass, is lowered according to the formula $m = 2\sqrt{\tilde{\lambda}}$. Thus, for a hole of depth -0.9 the stability line is lowered to $m = 0.6324$. In such a case all the Q-balls that can be obtained in the initially allowed frequency range will be unstable in the hole even when the Q-ball has zero velocity. This is clearly seen from figure 2 and this has been confirmed by our numerical simulations. In order to understand how much the Q-ball is affected by a hole as deep as -0.9, we have placed a Q-ball with $\omega = 1.9$, at rest, at $x = -14.0$ (i.e. close to the hole which is located at $-10 < x < 10$). As the times evolves the tail of the Q-ball interacts with the hole and generates many smaller Q-balls inside the hole. This can be seen in figure 5.

The number of smaller Q-balls which are produced inside the hole keeps on increasing and finally, after some time, settles to a nearly constant number. We have found that for each Q-ball the number of the small Q-balls produced inside the hole depends on how deep the hole is. Table 2 summarizes our results. It presents the number of smaller Q-balls created inside the hole for various hole depths when the initial Q-ball had $\omega = 1.9$ and, as before, was located at $x = -14$. For other values of ω the results were similar although as for lower

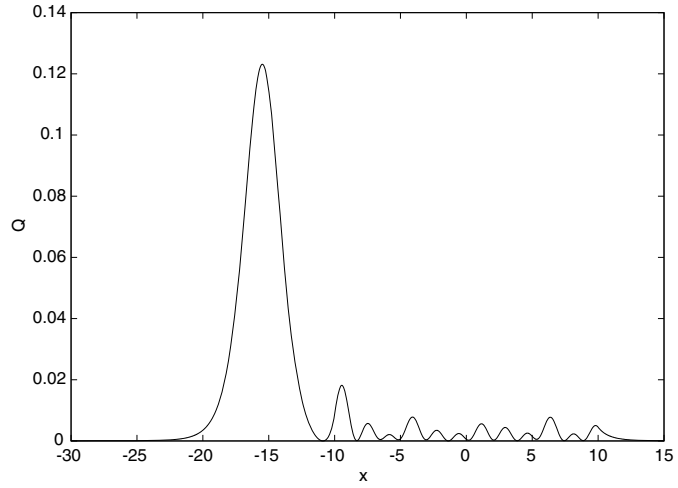

Figure 5. The Q-ball Q with $\omega = 1.9$ creating smaller Q-balls in the hole of depth -0.9.

Table 2. Number of Q-balls inside a hole for various hole depths.

	λ_0	No. of the Q-balls in the hole
	-0.9	12
	-0.6	10
$\omega = 1.9$	-0.5	9
	-0.3	7
	-0.2	5

values of ω the charge and energy were larger (see figure 1) and so the process of reaching the equilibrium was slower.

So, in situations where there are some Q-balls created inside the hole, the hole is not passive as was the case with a barrier but rather becomes a charged hole with a very complicated structure especially when there are many small Q-balls that had been produced inside it.

The force between a Q-ball and a hole is not very simple any more, as was the case for topological solitons. Again, it is the stability condition which, when violated, gives rise to this difference. We have found that when the stability condition is satisfied (and no small Q-balls are generated) the force between a Q-ball and a hole is attractive. This corresponds to what was seen for a topological soliton in the presence of holes. In the Q-ball case, however, we have found that, in general, the interaction can be described as corresponding to

- a purely attractive force,
- a purely repulsive force,
- a mixed force.

A purely attractive force has been observed when a Q-ball is stable or when a Q-ball may be unstable but has not been distorted too much by the presence of the hole. This can happen when the hole is shallow and the charge of the Q-ball is large. However, when the hole is deep and the Q-ball gets distorted, its tail develops many small Q-balls inside the hole and the force becomes repulsive. This repulsion then prevents the Q-ball from falling into the hole.

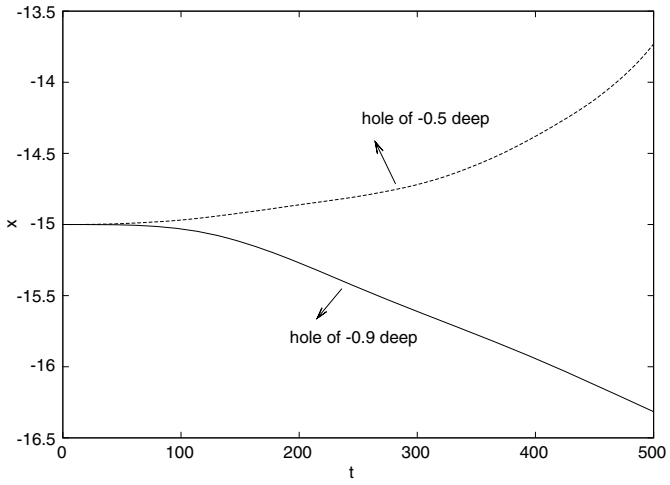

Figure 6. Plots of the time dependence of the position of a Q-ball with $\omega = 1.5$, $u = 0$, placed near holes of depth -0.5 and -0.9

Figure 6 presents the plots of the time evolution of two unstable Q-balls with frequency $\omega = 1.5$ placed, at rest, close to the holes of depth -0.5 and -0.9. We plot the positions of the 'parent' Q-balls as the scattering, in each case, generates small Q-balls in the hole. We note that while the shallower hole attracts the Q-ball, the opposite is the case for a deeper hole. This repulsion is due to the greater distortion of the Q-ball by the hole resulting in more small Q-balls in the hole which in turn changes the attraction into the repulsion.

In some of our simulations we have also observed that an unstable Q-ball could be, initially, attracted by the hole and then repelled by it. This occurs when the hole is not very deep and the tail of the Q-ball requires some time to generate the smaller Q-balls inside the hole. In this case, before generating these small Q-balls, the 'parent' Q-ball behaves as a normal soliton, i.e. is attracted by the hole. However, when the tail has already generated sufficient number of little Q-balls in the hole the repulsive force begins to dominate. Figure 7 describes such a case. It presents the plot of the position of a 'parent' Q-ball with $\omega = 1.9$ when the hole is of depth -0.125.

The above-mentioned results suggest that one should try to explain them in terms of the forces between Q-balls. Not much is known about such forces. In [15] some results are given; in particular, they show that two Q-balls with the same frequency ω attract each other if their relative phase θ is 0 and repel if $\theta = \pi$. In our case, the frequencies are different and so the forces (between the 'parent' Q-ball and it 'offspring') become effectively time dependent.

Given this situation we have performed further numerical studies. Thus we have placed Q-balls of frequency $\omega = 1.5$ and 1.9 far away from the hole of depth -0.9 and sent them with velocities 0.1 towards the hole. Both Q-balls moved towards the hole and when their tails reached the hole they started generating small Q-balls inside it. The small Q-balls inside the hole had various frequencies and so interacted with each other and with their 'parents'. These interactions amongst the 'baby' Q-balls let them oscillate inside the hole and ultimately led to the repulsion of the 'parent' Q-ball. We note that the Q-ball with $\omega = 1.5$ gets nearer to the hole but ultimately is reflected with a higher velocity than the Q-ball of $\omega = 1.9$. This can be partly understood by noting that although both Q-balls are unstable the one with $\omega = 1.5$ has a higher charge and hence requires a longer time for its tail to generate the Q-balls inside the hole. But once they are there their repulsion is stronger.

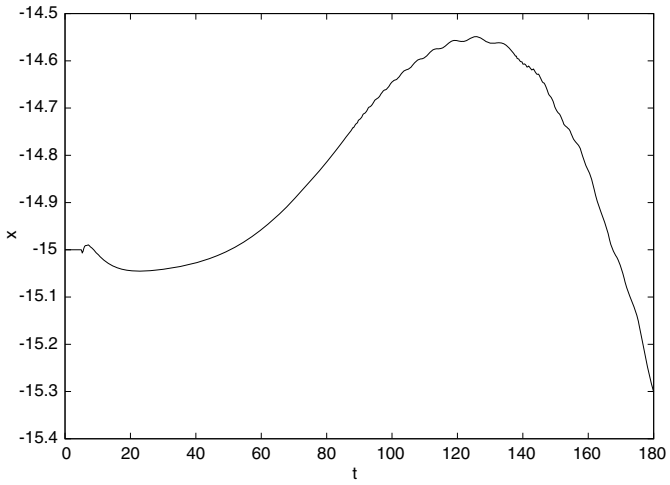

Figure 7. The dependence of the position of a 'parent' Q-ball with $\omega = 1.9$, $u = 0$, placed at rest close to a hole of depth -0.125.

Table 3. Dependence of $u_{\rm cr}$ on ω in a hole of depth -0.1.

ω	$u_{\rm cr}$
1.5	∼0.025
1.55	∼0.043 85
1.6	∼0.0445
1.65	∼0.072

If we increase the velocity of the Q-balls, their tails develop a smaller number of 'baby' Q-balls as if such Q-balls were more stable. In fact, this is not the case; a Q-ball moving with a higher speed is less stable but its interaction time with the hole gets shorter. Thus a Q-ball with $\omega = 1.9$, sent with velocity 0.95, has too little time to generate many 'baby' Q-balls inside it and gets through the hole without much distortion.

If we consider a shallow hole the stable Q-ball behaves very much like a topological soliton. So it moves along a well-defined trajectory and as it approaches the hole it speeds up. If the Q-ball has enough energy it comes out at the other end of the hole having generated very tiny radiation, otherwise it gets trapped in the hole. Figure 8 presents the plot of the time dependence of the position of a Q-ball with $\omega = 1.5$ sent towards the hole of depth -0.1 with velocity just below its critical value for transmission (in this case $u = 0.023$).

For a velocity slightly larger we observed the transmission. Hence the critical velocity for transmission is close to 0.024. Next we looked at the dependence of this critical velocity on the frequency of the Q-ball (i.e. its ω). Our results are presented in table 3.

As can be seen from the table the critical velocities increase as the charge Q decreases. The observed irregularities prevent us from drawing too detailed conclusions. Clearly, the exact values depend on the details of the interaction with the hole (the same phenomenon was observed for topological solitons—see [7]).

However, some information can be drawn from the fact that for a hole of depth -0.1 the stability line is lowered from $m = 2$ down to $m = 1.89$. As can be seen from figure 9 this

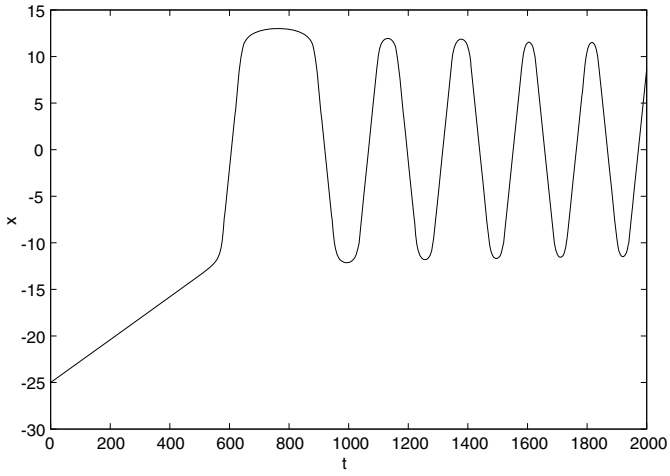

Figure 8. Time dependence of the position of a Q-ball with $\omega = 1.5$ sent towards the hole of depth -0.1 with velocity $u = 0.023$.

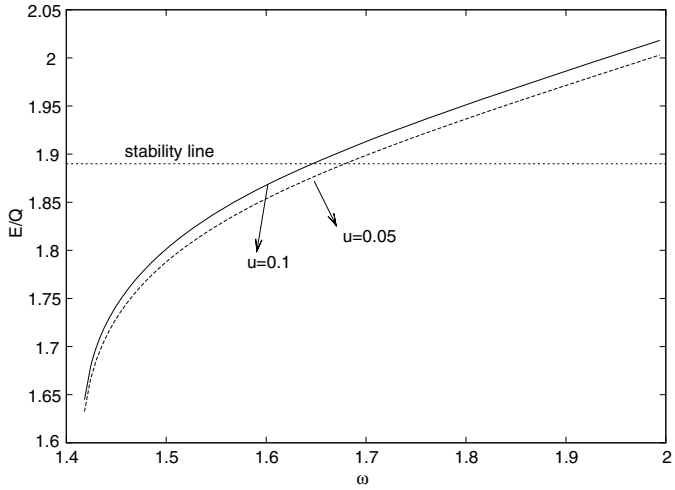

Figure 9. The stability line for a hole of depth -0.1.

affects the critical velocities for $\omega = 1.7$ and larger. Looking at figure 9 we note that, as the velocity increases, fewer Q-balls (with higher ω) are stable. Thus a Q-ball with $\omega = 1.65$ has as its critical velocity $u_{\rm cr} \sim 0.07$ which is just below the intersection point. However, for a Q-ball of frequency 1.7 and above we would expect its critical velocity to be greater than the one for $\omega = 1.65$ and hence such Q-balls will not be stable. This is, in fact, what has been observed in our numerical simulations. So, all velocities that lie above the intersection point would make the Q-balls unstable. Such Q-balls would generate 'baby' Q-balls and would not be transmitted. Hence, in such cases we would not have critical velocities. To be specific the critical velocity for a Q-ball with $\omega = 1.65$ is $u \sim 0.075$ and so at this velocity the intersection point is at $\omega = 1.664$. As $\omega = 1.65$ is below the stability line the Q-ball is stable and it has a critical velocity.

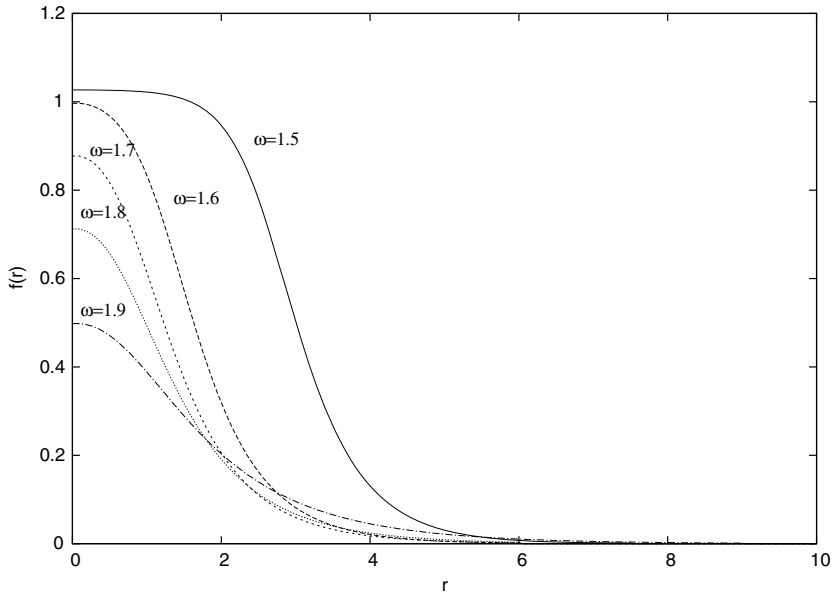

Figure 10. The numerically determined profiles functions f for $\omega = 1.5, 1.6, 1.7, 1.8, 1.9$.

5. Q-ball scattering in (2+1) dimensions

Next we consider the scattering of Q-balls in two spatial dimensions. As before we consider their behaviour in the presence of various potential obstructions.

We return to equation (1) and note that this time the index μ takes the values $\mu = 0, 1, 2$. The field equation becomes

$$\ddot{\Phi} - \nabla^2\Phi + 2\Phi\tilde{\lambda}(2 - 4|\Phi|^2 + 3|\Phi|^4) = 0, \tag{27}$$

where $\nabla^2 = \partial_x^2 + \partial_y^2$. The Q-ball ansatz becomes

$$\Phi(r, t) = f(r)\exp(\mathrm{i}\omega t), \tag{28}$$

where $r = \sqrt{x^2 + y^2}$. Equation (10) for the profile field f now becomes

$$\frac{\mathrm{d}^2 f}{\mathrm{d}r^2} + \frac{1}{r}\frac{\mathrm{d}f}{\mathrm{d}r} + \omega^2 f - 2\tilde{\lambda} f(2 - 4f^2 + 3f^5) = 0. \tag{29}$$

Here, as before, $\tilde{\lambda} = 1 + \lambda_0$.

As before the profile functions f were determined numerically. Figure 10 presents the plots of these profiles for various values of ω in the allowed range, i.e. $\sqrt{2} < \omega < 2$. Having found the static Q-balls we have boosted them along the x-axis by performing the appropriate Lorentz transformation, i.e.:

$$x' = \gamma(x - x_0 - ut), \qquad y' = y, \qquad t' = \gamma(t - u(x - x_0)), \tag{30}$$

where, as usual, $\gamma = \frac{1}{\sqrt{1-u^2}}$. This allows us to study the interactions of Q-balls as they, initially, move along the x-axis.

We have considered various potential obstructions. Most of our simulations have involved circular obstructions of radius $R = 5$. They were centred at (x_0, y_0). Looking at the profiles in figure 10 we note that for some ω's the Q-ball would not easily fit into the hole. However,

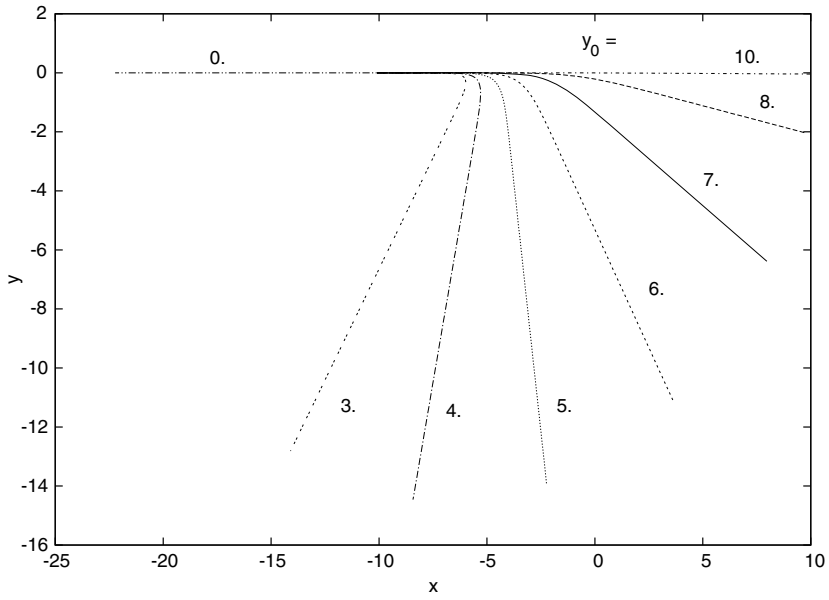

Figure 11. Q-ball scattering from barriers placed at various positions along the y-axis; $\omega = 1.75$.

in this work we have been primarily interested in the main aspects of the dynamics external to the holes—so for this such holes were sufficient. In our simulations we used a grid containing 300^2 points with $\mathrm{d}x = 0.1$, $\mathrm{d}y = 0.1$ and $\mathrm{d}t = 0.02$. Thus, the size of the grid and the size of the hole allowed us to study the dependence on the impact parameter of the scattering without having to worry about the edge effects.

5.1. Q-ball scattering on barriers in (2 + 1) *dimensions*

The scattering of Q-balls on barriers in (1 + 1) dimensions, discussed in the previous sections, has given a clear confirmation of a particle-like nature of Q-balls. This is further supported by our results on the scattering in (2 + 1) dimensions. As we have seen, the basic forces are repulsive and for each barrier there is a critical velocity above which the Q-ball gets transmitted over the barrier. In (2 + 1) dimensions, this force is also repulsive but this time the behaviour depends also on the impact parameter of the scattering.

To study this we have looked at the scattering of a Q-ball on a series of potential barriers whose position was varied along the y-axis (so that the scattering took places at different impact parameters). In figure 11, we present plots of the trajectories of Q-balls with $\omega = 1.75$ sent with velocity 0.1 at barriers of height 0.9 placed at $(0, y_0)$ for $y_0 = 0, 3, \ldots, 10$.

The plots also indicate that the Q-ball is deflected by the barrier before it reaches it with its centre. Hence the deflection is due to the interaction of the Q-ball tail. The deflection angle depends on the impact parameter. As the hole has radius 5 and the size of the Q-ball is essentially 5 we expect very little deflection when $y_0 \sim 10$. This is, in fact, what is seen from the plots in figure 11. As the impact parameter decreases the angle of reflection increases and at zero impact parameter the Q-ball is fully reflected. Table 4 presents the deflection angles seen in the scatterings.

Table 4. Observed deflection angles for some values of the impact parameter.

y_0	θ°
10.0	0.5189
8.0	8.555
7.0	31.955
6.0	57.84
5.0	81.159
4.0	103.63
3.0	123.68
0.0	180

These angles have been calculated numerically by using

$$\theta = \tan^{-1}\left(\frac{u_y}{u_x}\right), \tag{31}$$

where u_x and u_y are the velocities along the x- and y- axes, respectively.

How do these results depend on the height of the barrier or the frequency of the Q-ball? Or on the velocity of the Q-ball?

We have performed further studies and have found that when a Q-ball is sent at higher speed, the deflection angle is smaller. This is clearly due to the fact that at higher velocity the Q-ball has more power to overcome the barrier and so gets nearer to the centre of the barrier. What about the dependence on the height of the barrier?

We note that the deflection angle is smaller for the smaller barrier; again, in this case the Q-ball gets nearer to the centre of the barrier. This behaviour has been observed for a Q-ball of frequency $\omega = 1.75$ sent from $y_0 = 7$ towards the barriers of height 0.5 and 0.9.

Furthermore, we have also found that the deflection angle increases with the decrease of the Q-ball charge (i.e. ω). We have observed such behaviour for two Q-balls (with $\omega = 1.75$ and 1.9) sent from $y_0 = 0.0$ with velocity 0.1 towards a barrier of height 0.9 located at $(x_0, y_0) = (0, 7.0)$. The deflection angles for the Q-balls with $\omega = 1.75$ and $\omega = 1.9$ are found to be 31.955 and 40.167, respectively.

5.2. Q-ball scattering on holes in (2 + 1) *dimensions*

We have also studied the Q-ball scattering on holes. Like in the (1 + 1)-dimensional case the whole process is more complicated than the scattering on barriers. As in the (1 + 1)-dimensional case the complications arise from the generation of 'baby' Q-balls in the hole and their repulsion. Also the smaller the velocity the more time the 'parent' Q-ball has for generating these 'baby' Q-balls.

This, coupled with the dependence on the impact parameter, makes the whole process very complicated. So here we present our preliminary results—leaving more detailed investigations for the future. However, these preliminary results are interesting enough to report them here.

First of all let us note that, like in the (1 + 1)-dimensional case, the overall force between the Q-ball and the hole can be repulsive, attractive or a mixture of these two and this depends on the velocity of the Q-ball, its charge and the position and the depth of the hole. This dependence is mainly due to the conditions of the stability of the Q-ball. When the Q-balls, during the process of the scattering, remain stable the force between them and the hole is purely attractive and the process resembles the scattering on the barriers except that this time the deflection is towards the hole.

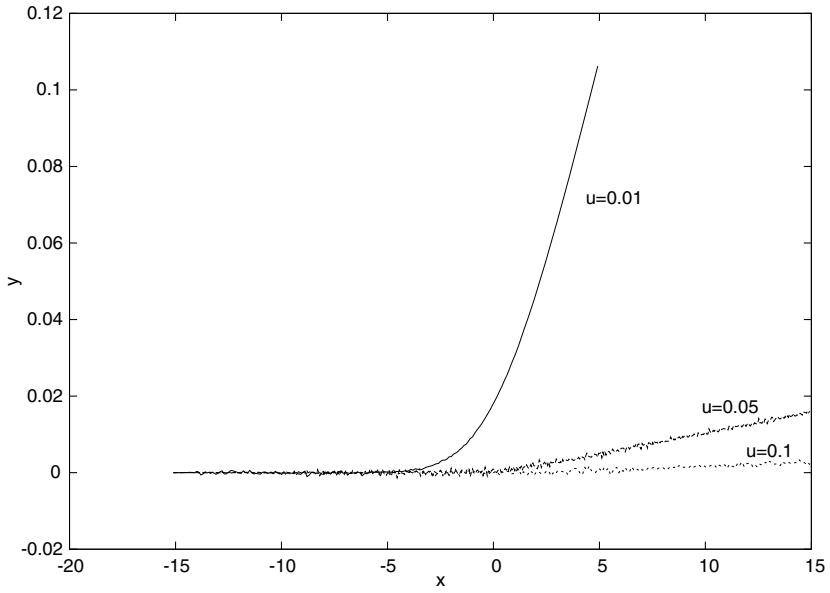

Figure 12. Trajectories of Q-balls ($\omega = 1.6$) sent with various incoming velocities for a hole of depth -0.9 located at $y_0 = 11.5$.

However, the behaviour depends on the initial velocity; the faster the Q-balls move the less they are deflected by the hole. Figure 12 presents the trajectories of three Q-balls (of $\omega = 1.6$) sent with velocities $u = 0.1, 0.05$ and 0.01 when the hole (of depth -0.9) was located at $(0.0, 11.5)$. The plots show very clearly that the force between the Q-ball and the hole is attractive but the deflection decreases with the increase in the speed of the Q-ball.

Next we report the results of our study of the dependence on the impact parameter. Figure 13 presents the trajectories of the Q-ball ($\omega = 1.6$) sent with velocity $u = 0.1$ at various impact parameters, i.e. $y_0 = 10$, 10.5, and 11. As expected, we see that the deflection increases as we decrease the impact parameter (when the Q-balls are sent with the same velocity).

As we decrease the impact parameter y_0 further, bringing the hole closer to the x-axis, the net interaction between the Q-ball and the hole ceases being purely attractive and becomes partially repulsive and partially attractive. This results in a complicated behaviour which is due to what we have seen in the one-dimensional scattering: the hole is no longer a passive object but rather a charged object (due to the 'baby Q-balls' that have been generated in the hole) and that affects the interaction.

Figure 14 presents the trajectories of two Q-balls (with $\omega = 1.6$) sent with velocities $u = 0.05, u = 0.2$ towards a hole located at $y_0 = 8.0$. From the figure one sees very clearly that initially the scattering of the Q-ball with velocity 0.2 is repulsive and later becomes attractive. Note the small scale of the y-axis which shows that the motion in the y-direction is very small. Hence, the behaviour is very sensitive to the values of various parameters (velocity or impact parameter). Furthermore, when a Q-ball is sent with a small velocity, it can interact with the hole earlier. At this stage the force is attractive and the Q-ball has not yet had the time to generate many 'baby' Q-balls in the hole. Thus the repulsive force is smaller or even disappears altogether and a purely attractive force is observed. From the figure one sees very clearly the repulsive force seen in the case of $u = 0.2$ disappears when the Q-ball velocity is decreased to $u = 0.05$ and that, in this latter case, the overall force is attractive.

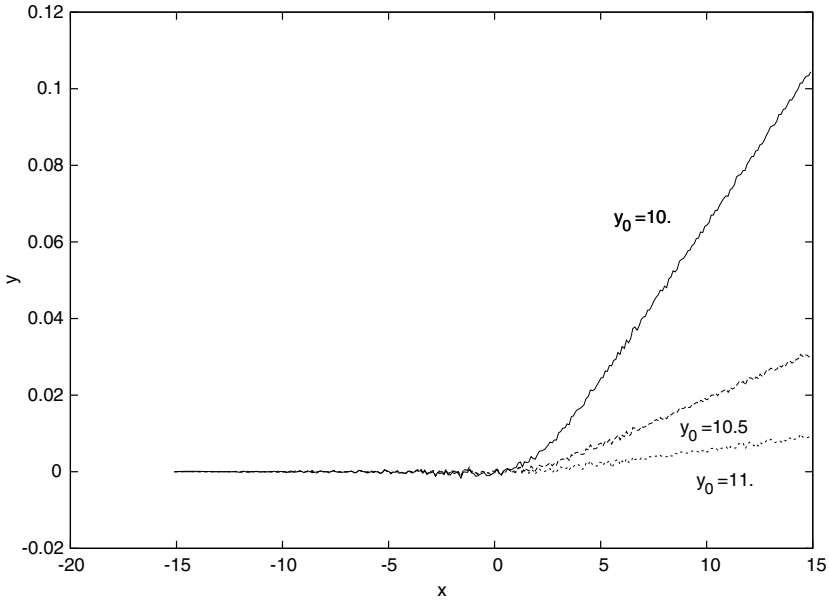

Figure 13. Trajectories of a Q-ball sent with velocity ($u = 0.1$) for a hole of depth -0.9 located at various impact parameters.

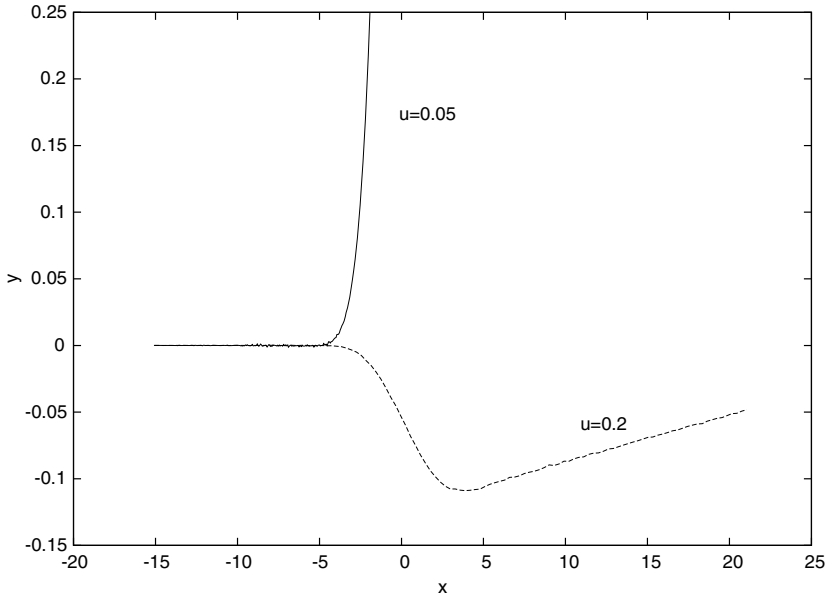

Figure 14. Trajectories of two Q-balls (of $\omega = 1.6$) sent with velocities $u = 0.2$ and $u = 0.05$ towards a hole of depth -0.9 located at $y_0 = 8.0$.

The magnitude and the type of the overall force between the Q-ball and the hole, when a Q-ball is sent with a certain speed and at a certain impact parameter, depends also on the charge of the Q-ball (i.e. ω). Figure 15 presents the trajectories of Q-balls of different charges

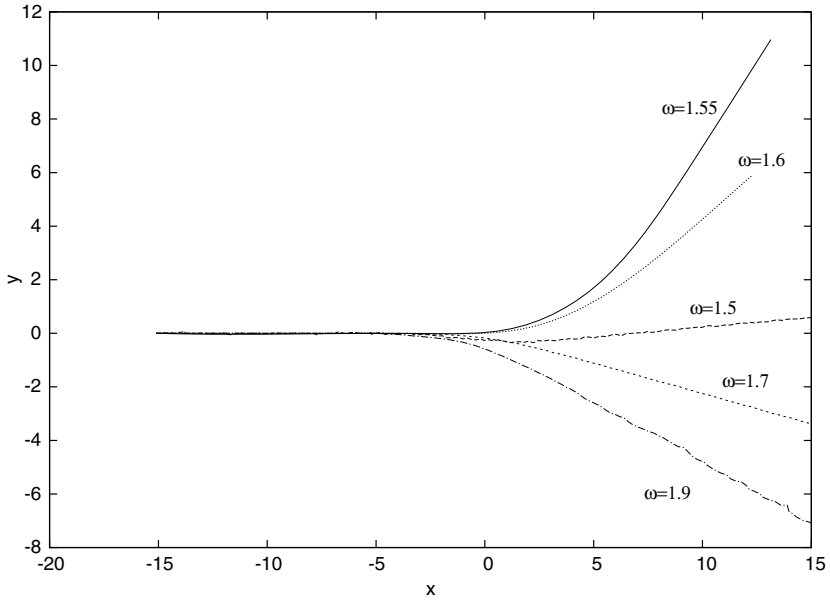

Figure 15. The trajectories of a Q-ball with $\omega = 1.5, 1.55, 1.6, 1.7, 1.9$ sent with $u = 0.1$, a hole of -0.9 depth located at $y_0 = 8.5$

(different ω) when each Q-ball was sent with velocity 0.1 and towards a hole of -0.9 located at $y_0 = 8.5$. We note a very strong dependence on the charge. Sometimes the trajectories are deflected towards the hole, for other ω they are deflected in the other direction. The amount of the deflection also depends strongly on ω. Clearly this is a complicated process which requires further investigation. One factor that certainly is partially responsible for this behaviour is the broadness of the profile functions. However, this broadness is basically monotonic (but not at the tail, see figure 10) so it is hard to predict how much charge (in the form of 'baby' Q-balls) get generated in the hole and how this affects the overall scattering properties. All this behaviour requires more detailed further investigation.

Finally, we have also checked, numerically, that the forces are independent of the overall helicity, that is the force does not depend on the sign of ω. The behaviour is independent of whether we send a Q-ball or an anti-Q-ball at a hole located at the same position. The dynamics also does not depend on the sign of the impact parameter, i.e. it is also still the same when a Q-ball is sent (with the same velocity) towards a hole located at a corresponding negative impact parameter.

As the forces between a Q-ball and a hole are attractive in the region of stability of the Q-ball all deflections can be cancelled if we send a Q-ball symmetrically in-between two holes. Then the only effect is a small attraction as the Q-ball approaches the line joining the holes followed by a repulsion. So, in this case the Q-ball behaves again like a point particle.

6. Conclusion

In this paper we have presented the results of our studies of the scattering of Q-balls on potential obstructions (in the form of potential barriers and holes) in (1 + 1) and (2 + 1) dimensions. In our work we have tried to compare our results with similar results for topological solitons. And in many cases the results were similar; however, some results were different as Q-balls

have some conditions that they have to satisfy to be stable. Moreover, as their charge is not quantized they can, in the interaction with obstructions, generate further small Q-balls (called 'baby' Q-balls in this paper).

We have found that in the barrier case the scattering of Q-balls resembled very closely the scattering of topological solitons. The scattering was very elastic. For each barrier there was a critical velocity below which the Q-ball was reflected and above which it was transmitted. What was surprising, at first sight, was that the value of this critical velocity did not depend on the charge of the Q-ball (i.e. it was independent of ω). As the scattering was very elastic we could estimate the value of this critical velocity by performing an energy analysis (i.e. by comparing the energy of a boosted Q-ball away from the barrier to the energy of Q-ball at rest at the top of the barrier). The results were in an excellent agreement with what was seen in the numerical simulations. This suggests that, indeed, the scattering is very elastic and the approximation of Q-balls by point-like particles is quite reliable.

For the scattering of Q-balls on potential holes the situation was slightly different as the stable Q-balls, when they fall into a hole can become unstable. This instability translates into the generation of 'baby' Q-balls which can then interact with their 'parent'.

We have performed detailed studies of the scattering of Q-balls on potential holes. When the Q-balls are stable, and remain stable in the hole, they, again, resemble topological solitons. In this case they can either fall into the hole and get trapped in it or pass through it with a slightly reduced velocity. The scattering is, again, quite close to being elastic although this time more radiation is produced than in the case of a barrier. However, when a Q-ball approaches the hole, especially when its parameters are close to the stability bounds, it produces small Q-balls in the hole. As the basic force between Q-balls can be of either sign (it depends on their relative phase) the 'baby' Q-balls then start interacting with each other and with the initial Q-ball. The overall interaction can now be attractive or repulsive and this depends on the parameters of the configuration (velocity and frequency of the Q-ball, the position and the height of the hole, etc).

In $(2+1)$ dimensions we have looked at the scattering of a Q-ball on a series of potential barriers whose position was varied along the y-axis. The Q-ball was deflected from the potential barrier. We have found that the deflection angle depended on the impact parameter, the height of the barrier, the velocity and the charge Q of the Q-ball.

We have also studied the interactions of stable Q-balls with the hole in $(2+1)$ dimensions at various impact parameters. We have found the expected deflection towards the hole although the trajectories of the 'parent' Q-ball were slightly irregular. This irregularity increased at the lower impact parameters and it depended also on the velocity of the Q-ball. When we studied the dependence of the impact parameter on the charge of the Q-ball (i.e. the frequency ω) we have found a surprising irregularity as shown in figure 15. For some frequencies the deflection was towards the hole, for some others away and it varied in magnitude in a very unpredictable way. Clearly the overall forces in this case are very finely balanced. It is clear that to get a good understanding of the scattering on a hole requires further work.

Acknowledgment

One of us (JHA) would like to thank P M Sutcliffe for a helpful discussion.

References

[1] Al-Alawi J H and Zakrzewski W J 2007 *J. Phys. A: Math. Theor.* **40** 11319–11331
[2] Al-Alawi J H and Zakrzewski W J 2008 *J. Phys. A: Math. Theor.* **41** 315206

[3] Kivshar Y S and Malomed B A 1988 *Phys. Lett.* A **129** 443–8
[4] Goldobin E, Malomed B A and Ustinov A V 2000 *Phys. Lett.* A **266** 67–75
[5] Klushin A M, Gelikonova V D, Numssen K, Borovitskii S I and Siegel M 2002 *Physica* C **372–376** 301–4
[6] Coleman S 1985 *Nucl. Phys.* B **262** 263
[7] Piette B and Zakrzewski W J 2007 *J. Phys. A: Math. Theor.* **40** 329–46
[8] Piette B and Zakrzewski W J 2007 *J. Phys. A: Math. Theor.* **40** 5995–6010
[9] Tsumagari M I, Copeland E J and Saffin P M 2008 Some stationary properties of a Q-ball in arbitrary space dimensions arXiv:0805.3233v2
[10] Battye R A and Sutcliffe P M 2000 *Nucl. Phys.* B **590** 329
[11] Lee T D 1981 *Particle Physics and Introduction to Field Theory* (London: Harwood)
[12] Multamaki T and Vilja I 1999 Analytic and numerical properties of Q-balls arXiv:hep-ph/9908446
[13] Axenides M, Komineas S, Perivolaropoulos L and Floratos M 2000 *Phys. Rev.* D **61** 085006
[14] Kusenko A 1997 *Phys. Lett.* B **405** 108
[15] Bowcock P, Foster D and Sutcliffe P M 2008 Q-balls, integrability and duality arXiv:0809.3895v1